Molecular Immunology 107 (2019) 29–40

Contents lists available at ScienceDirect

Molecular Immunology

journal homepage: www.elsevier.com/locate/molimm

Blockade of YAP alleviates hepatic fibrosis through accelerating apoptosis and reversion of activated hepatic stellate cells

Hai-xia Yu[a,b,c], Yao Yao[a,b,c], Fang-tian Bu[a,b,c], Yu Chen[a,b,c], Yu-ting Wu[a,b,c], Yang Yang[a,b,c], Xin Chen[a,b,c], Yan Zhu[a,b,c], Qin Wang[a,b,c], Xue-yin Pan[a,b,c], Xiao-ming Meng[a,b,c], Cheng Huang[a,b,c,*], Jun Li[a,b,c,*]

[a] The Key Laboratory of Major Autoimmune Diseases, Anhui Province, Anhui Institute of Innovative Drugs, School of Pharmacy, Anhui Medical University, Hefei, China
[b] The Key Laboratory of Anti-inflammatory of Immune Medicines, Ministry of Education, Hefei, China
[c] Institute for Liver Diseases of Anhui Medical University, Hefei, China

ARTICLE INFO

Keywords:
Hepatic fibrosis
YAP
Wnt/β-catenin
Reversion
VP

ABSTRACT

Yes-associated protein (YAP) is a significant downstream protein in the Hippo signaling pathway with important functions in cell proliferation, apoptosis, invasion and migration. YAP also plays a role in the progression and development of various liver diseases. In hepatic fibrosis development and reversion, the proliferation and apoptosis of activated hepatic stellate cells (HSCs) play a critical role. However, the contribution of YAP to hepatic fibrosis progression and reversion and the underlying mechanism have not been investigated. Here we investigated the expression and function of YAP in the proliferation and apoptosis of activated HSCs. We found that YAP expression was increased in liver fibrosis tissues from CCl_4-induced model mice and restored to normal level after stopping CCl_4 injection and 6 weeks of spontaneously recovery. YAP expression was elevated in HSC-T6 cells treated with TGF-β1 and recovered after MDI treatment. Silencing of YAP inhibited the activation and proliferation of HSC-T6 cells stimulated by TGF-β1. In addition, the apoptosis of activated HSC-T6 cells silenced for YAP was slightly enhanced. Furthermore, over-expression of YAP repressed the reversion of activated HSC-T6 cells mediated by MDI reversal. We found that HSC-T6 cells activated by TGF-β1 showed higher levels of nuclear YAP compared with MDI-treated cells, indicating that YAP was activated in HSC-T6 cells treated by TGF-β1. We also found that loss of YAP attenuated Wnt/β-catenin pathway activity in activated HSC-T6 cells. Treatment of VP, an inhibitor of the YAP-TEAD complex, reduced both activation and proliferation of HSC-T6 cells and increased apoptosis. Together these results indicated that reduced expression of YAP contributes to acquisition of the quiescent phenotype in HSCs. Our results suggest that YAP may be a useful target in HSCs activation and reversion.

1. Introduction

Hepatic fibrosis, a serious public health problem, is a wound-healing process caused by various factors such as hepatitis virus, toxins, drugs, ethanol and autoimmune disorders. Hepatic fibrosis often leads to excessive extracellular matrix (ECM) deposition in liver. Hepatic stellate cell (HSC) activation, the key event of hepatic fibrogenesis, plays an important role in the up-regulation of α-smooth muscle actin (α-SMA) and abundant production and secretion of ECM such as types I collagen (Col1a1), ultimately resulting in the deposition of fibrous tissue and scar formation, in addition, the expression of desmin is strongly up-regulated (Parola et al., 2008; Zhang et al., 2018). When challenged with liver injury, quiescent HSCs (qHSCs) are activated and differentiate to a myofibroblastic phenotype characterized by the loss of retinoids and lipid droplets. Many pro-fibrogenic growth factors and cytokines initiate myofibroblastic differentiation, such as transforming growth factor-β1 (TGF-β1) and platelet-derived growth factor (PDGF). Therefore, TGF-β1 and PDGF have been used to activate HSCs *in vitro*. At present, inhibiting the activation of qHSCs is a crucial therapeutic method for hepatic fibrosis. Over the past decade, many studies

Abbreviations: YAP, Yes-associated protein; HSCs, hepatic stellate cells; TGF-β1, transforming growth factor-β1; MDI, adipocyte differentiation cocktail; VP, Verteporfin; TEAD, transcriptional enhancer factor with TEA/ATTS domain; ECM, extracellular matrix; PDGF, platelet-derived growth factor; Col1a1, type I collagen; α-SMA, α-smooth muscle actin; CTGF, connective tissue growth factor

* Corresponding authors at: School of Pharmacy, Anhui Medical University, 81 Meishan Road, Hefei, Anhui Province, 230032, China.
E-mail addresses: huangcheng@ahmu.edu.cn (C. Huang), lj@ahmu.edu.cn, yuhaixia0505@126.com (J. Li).

https://doi.org/10.1016/j.molimm.2019.01.004
Received 3 July 2018; Received in revised form 20 December 2018; Accepted 4 January 2019
Available online 11 January 2019
0161-5890/

demonstrated that hepatic fibrosis could be reversed, not only in experimental models of liver fibrosis, but also in humans (Ellis and Mann, 2012). In 2005, She and co-workers showed that activated HSCs could undergo morphologic and biochemical reversal to qHSCs by treatment with an adipocyte differentiation cocktail (MDI). MDI has thus been used to create a model for liver fibrosis reversion *in vitro* to research the underlying mechanism of hepatic fibrosis reversion (She et al., 2005). Although much research has been focused on the mechanism and therapeutic strategy for hepatic fibrosis, the identification of successful treatment approaches for hepatic fibrosis has remained elusive.

The Hippo pathway, originally identified in Drosophila (Yu FX and Guan, 2015), is a crucial signaling pathway that is highly conserved in mammals. YAP (Yes-associated protein), a 65 KDa protein, is a transcriptional coactivator and the major downstream effector of the Hippo signaling cascade. The YAP gene is located in the human chromosome 11q22 genomic region and encodes the YAP protein, which binds to the SH3 domain of the Yes tyrosine kinase (Sudol et al., 1995). YAP has two informs including YAP1 and YAP2, which both contain a proline rich domain, WW domain, coiled-coil domain, and a PDZ-binding motif formed by the four C-terminal amino acids (LTWL) (Ou et al., 2017). Under physiological conditions, the Hippo pathway is activated and YAP is phosphorylated and thus retained in the cytoplasm (Halder and Johnson, 2011; Oh and Irvine, 2010). However, when the Hippo pathway is inactivated, non-phosphorylated YAP can translocate into the cell nucleus to activate downstream genes expressions, such as connective tissue growth factor (CTGF) and ankyrin repeat domain 1 (Ankrd1), and affect cell biological functions (Shi et al., 2017). YAP plays important roles in cell proliferation, apoptosis, migration, differentiation and invasion (Harvey et al., 2013; Li et al., 2017; Liu et al., 2017). Li et al demonstrated that YAP promoted chronic myeloid leukemia cell proliferation, indicating that inhibition of YAP may be a potential therapeutic approach in chronic myeloid leukemia (Li et al., 2016). YAP also plays important functions in various liver diseases, such as hepatocellular carcinoma, non-alcoholic fatty liver and liver regeneration after partial hepatectomy (Wu et al., 2016; Grijalva et al., 2014; Machado et al., 2015). YAP is also involved in hepatocyte fate change in the face of different cellular stress (Miyamura et al., 2017). Some studies also found that YAP levels increased and YAP underwent nuclear localization at an early time point during the activation of HSCs, indicating that YAP may function at the earliest stage of HSC activation (Mannaerts et al., 2015). Another report showed that YAP could mediate HSC activation and proliferation after liver ischemia/reperfusion (Konishi et al., 2018). However, the potential functions and mechanism of YAP in hepatic fibrogenesis and reversal have not been fully addressed.

Many studies have shown that the Wnt/β-catenin pathway is activated in hepatic fibrosis and β-catenin is a crucial pro-fibrotic factor (Tan et al., 2011). Our preliminary study also revealed that the Wnt/β-catenin pathway was initiated and the downstream target gene expressions were increased in a CCl_4-induced liver fibrosis mouse model as well as HSC-T6 cells activated by TGF-β1 (Cai et al., 2016). Several studies have demonstrated interactions between the Hippo/YAP pathway and the Wnt/β-catenin pathway in some diseases, such as glioma and ulcerative colitis (Wang et al., 2017; Deng et al., 2018; Bejoy et al., 2018). In chondrocyte differentiation, YAP suppressed the differentiation of mouse chondroprogenitor ATDC5 cells through activating the Wnt/β-catenin signaling pathway. Furthermore, when YAP was over-expressed, the Wnt/β-catenin signaling pathway was robustly activated (Yang et al., 2017). Moreover, Yang et al demonstrated that the expression of YAP in osteosarcoma cell lines was increased, and blockade of YAP could prevent proliferation and colony formation activities of osteosarcoma cells. YAP knockdown decreased expressions of Wnt signaling pathway target genes, such as C-myc and cyclin D1 genes (Yang et al., 2014). Other reports indicated that p-YAP in the cytoplasm could interact with β-catenin and lead to β-catenin retention (Imajo et al., 2012). The interaction between nuclear YAP and β-catenin promoted Sox2 and Snai2 gene expression to affect heart growth (Heallen et al., 2011). However, whether the Hippo/YAP pathway and Wnt/β-catenin pathway interact in liver fibrosis development and reversal is still unclear.

Here, we investigated the expression of YAP in liver tissue and HSC-T6 cells. We explored the effect of YAP on HSC-T6 cell activation by TGF-β1 treatment and reversion by MDI treatment. We also studied the interaction between the YAP and Wnt/β-catenin pathway. Our findings help enhance our understanding on the progression and reversion of hepatic fibrosis and uncover the link between the YAP and Wnt/β-catenin pathway.

2. Material and methods

2.1. Animals and treatments

Male C57BL/6 mice (18–20 g) were purchased from the experimental Animal Center of Anhui Medical University. The animal experiments were reviewed and approved by the University Animal Care and Use Committee. Mice were randomly divided into three groups (vehicle group, hepatic fibrosis model group and hepatic fibrosis recovery group, n = 15/group). The hepatic fibrosis mice were generated by intraperitoneal injection of 10% CCl_4 in olive oil for 4 weeks (2 ml per kg, twice per week). Mice in the vehicle group were injected with the same volume of olive oil. The mice in the reverse group were also injected with 10% CCl_4 for 4 weeks, and after the cessation of injection for 6 weeks, the model of hepatic fibrosis reversal was successfully established. Mice were given a single dose of VP (100 mg/kg) 4 h before the last injection.

2.2. Primary HSCs isolation and HSC-T6 cells culture

Primary HSCs were isolated from mice in all three experimental groups according to previous studies (Cai et al., 2016; Si et al., 2008). The HSC-T6 cell line was acquired from Shanghai Fumeng Gene Biological Corporation (Shanghai, China). HSC-T6 cells were maintained in Dulbecco's modified Eagle's medium (DMEM, Keygen, China) supplemented with 5% (v/v) fetal bovine serum (FBS, Every Green, China), 100 U/ml penicillin and 100 mg/ml streptomycin and cultured at 37 °C with 5% CO_2. For HSC activation *in vitro*, HSC-T6 cells at 80% confluence were treated with TGF-β1 (10 ng/ml, Peprotech, USA) for 24 h. To reverse activated HSC-T6 cells, cells were treated with MDI (0.5 mM isobutylmethylxanthine, 1 μM dexamethasone and 167 nM insulin; all from Sigma-Aldrich, St. Louis, MO, USA) with 5% FBS for 48 h.

2.3. Total RNA isolation and real-time quantitative PCR (RT-qPCR)

Total RNA was extracted from liver tissue and HSC-T6 cells using Trizol (Invitrogen, USA), and cDNA was synthesized using the PrimeScript® RT reagent kit (Takara, Japan) according to the manufacturer's instructions. Col1a1, α-SMA, YAP, and CTGF mRNA expressions were detected by using Takara SYBRGreen PCR Kit (Takara) in the Pikoreal 96 real-time PCR system (Thermo Scientific, USA). All prime sequences (Sangon Biotech, China) listed in Table 1. All experiments were performed in triplicate.

2.4. Western blot analysis

Proteins were extracted from liver tissue and HSC-T6 cells using RIPA lysis buffer (Beyotime, China), and the protein concentration was measured using a BCA protein assay kit (Beyotime). The samples were mixed with loading buffer, and the mixture was boiled at 100 °C for 10 min. Protein samples were separated on a SDS-PAGE gel and transferred to PVDF membranes (Millipore Corp, Billerica, MA, USA). The PVDF membranes were blocked with TBST containing 5% skim milk for 3 h at room temperature and then washed three times in TBST. The

Table 1
Primes used in RT-qPCR.

Gene	Forward prime (5'-3')	Reverse prime (5'-3')
Mouse		
Col1a1	TCCCTGGAATGAAGGGACAC	CTCTCCCTTAGGACCAGCAG
α-SMA	GCACCTGGATCATTGCTTCC	TCCTTGGAAGTACTGCCGTT
YAP	GAGGGACTCCGAATGCAG	CGAGAGTGATAGGTGCCACTG
GAPDH	AATGTGTCCGTCGTGGATCT	AGACAACCTGGTCCTCAGTG
Rat		
Col1a1	GATCCTGCCGATGTCGCTAT	TGTAGGCTACGCTGTTCTTGCA
α-SMA	CGAAGCGCAGAGCAAGAGA	CATGTCGTCCCAGTTGGTGAT
YAP	TCGGTACTGGCCTGTCGCGA	CGTGCCCATGAGGCTTCGCA
CTGF	AAGACCTGTGGGATGGGC	TGGTGCAGCCAGAAAGCTC
β-actin	CACCCGCGATACAACCTTC	CCCATACCCACCATCACACC

PVDF membranes were then incubated with primary antibody overnight, followed by incubation with secondary antibodies (1:10000, ZSGB-Bio, China) for 1 h at room temperature. The protein bands were detected by an enhanced chemiluminescent kit (ECL-plus, Thermo Scientific). Primary antibodies anti-YAP, anti-BAX, anti-BCL-2, anti-caspase-3, anti-β-catenin, anti-C-myc and anti-cyclinD1 (all rabbit polyclonal from Cell Signaling, USA) were diluted 1:1000; anti- Col1a1, anti-α-SMA and anti-β-actin (all rabbit polyclonal from Boster, China) were diluted 1:500; and anti-histone-H3 (rabbit polyclonal, Protein Tech, China) was diluted 1:500.

2.5. RNA interference analysis

HSC-T6 cells were transfected with small interfering RNA (siRNA) using Lipofectamine2000 (Invitrogen) and Opti-MEM (Gibco, USA). After 6 h, the Opti-MEM was replaced by DMEM and cells were activated with TGF-β1 at 10 ng/ml. The sequences of siRNAs were as follows: YAP-siRNA, 5′-GGAGAAGUUUACUACAUAATT-3′ and 5′-UUAUGUAGUAAACUUCUC CTT-3′; and scrambled-siRNA, 5′-UUCUCCGAACGUGUCACGUTT-3′ and 5′-ACGUGACACGUUCGGAGAATT-3′ (GenePharma Corporation, China).

2.6. Cell proliferation assay

HSC-T6 cell proliferation was determined using the Cell Counting Kit-8 (CCK-8) assay (BestBio, China). HSC-T6 cells (5×10^3 cells/well) were seeded in 96-well culture plates. After attachment, the cells were transfected with scrambled-siRNA or YAP-siRNA. At 24 h later, 10 μl CCK-8 were added to each well and cells were cultured at 37 °C for 3 h. Absorbance was detected at 450 nm using the Thermomax microplate reader (Bio-TekEL, USA).

2.7. Cell cycle analysis

The cell cycle was examined using the Cell Cycle and Apoptosis Analysis Kit (Beyotime). Transfected cells were trypsinized, washed by cold PBS and then fixed in 1 ml 70% cold ethanol at 4 °C overnight. After centrifugation, the cells were washed once and incubated with 0.5 ml of propidium iodide (PI) staining buffer containing 200 mg/ml RNase A and 50 μg/ml PI at 37 °C for 30 min in the dark. A flow cytometer (Beckman, USA) was used to analyze the cell cycle, and data were analyzed using ModFit software (Verity Software House, USA).

2.8. Cell apoptosis analysis

Cell apoptosis was detected using the Annexin-V-FITC Apoptosis Detection Kit (BestBio). Transfected HSC-T6 cells were trypsinized, collected in 15 ml centrifuge tubes and washed twice with cold PBS. The cells were resuspended in 400 μl Annexin V binding buffer and then 5 μl Annexin V-FITC and PI were added. The cell apoptosis rate was detected using a flow cytometer (BD Biosciences, USA) within 1 h. Apoptosis data were analyzed using FlowJo software (TreeStar, USA).

2.9. Plasmid transfection of HSC-T6 cells

HSC-T6 cells were seeded in 6-well-plates. After attachment, the cells were transfected with SV40-YAP (GeneChem, China) or SV40-Control *via* using Lipofectamine2000 and Opti-MEM for 6 h. Opti-MEM was then replaced by DMEM and cells were activated by TGF-β1 (10 ng/ml) for 24 h. After activation, the cells were cultured in MDI for 48 h as described above and then protein and RNA were extracted for experiments.

2.10. Immunofluorescence staining

Frozen liver tissue sections of mice were blocked with 10% bovine serum albumin (BSA) at 37 °C for 25 min to avoid unspecific staining. Anti-YAP (1:100), anti-α-SMA (1:800) or anti-desmin (1:400, Boster) diluted in 1% BSA were added to sections and incubated at 4 °C overnight. Sections were then incubated with a mixture of TRITC-conjugated secondary antibody (1:80, ZSGB-Bio) and FITC-conjugated secondary antibody (1:80, ZSGB-Bio) diluted in 1% BSA in the dark at 37 °C for 1 h. The stained sections were examined using inversion fluorescence microscopy.

2.11. Cytoplasmic and nuclear protein extraction

Cytoplasmic and nuclear proteins were extracted using a nuclear protein extraction kit (BestBio). Briefly, liver tissues were sheared in cold PBS, and HSC-T6 cells were collected and washed twice with cold PBS. Solution A (200 μl), including 1 μl protease inhibitor mixture and 1 μl phosphatase inhibitor, was added to the samples and then the samples were mixed for 30 min by shaking. After centrifugation, the supernatant was removed as the cytoplasmic protein sample. The precipitated material was washed with cold PBS and mixed with solution B (200 μl), which included 1 μl protease inhibitor mixture and 1 μl phosphatase inhibitor. After 40 min shaking, the supernatant was extracted as the nuclear protein sample.

2.12. Verteporfin (VP) treatment and MTT assay

VP (MedChemExpress, China), an inhibitor of the YAP-TEAD complex, was diluted to different concentrations using DMSO. The cytotoxicity of VP was assessed by 3-(4, 5-dimethylthiazol-2-yl)-2, 4-diphenyl-tetrazolium bromide (MTT, Sigma) assays. HSC-T6 cells were plated in a 96-well culture plate. After adherence, cells were cultured with various concentrations of VP. At 24 h later, 20 μl of 5 mg/ml MTT was added to each well. After 4 h, the medium was replaced with 150 μl DMSO. The absorbance was detected at 490 nm using a Thermomax microplate reader (Bio-TekEL). An optimal VP concentration was selected to stimulate the cells and TGF-β1 was added 6 h later.

2.13. Statistical analysis

All data are shown as mean ± SEM and were calculated using GraphPad Software. The difference of two groups was confirmed by Student's *t*-test and the difference of multiple groups was defined through one-way ANOVA. Statistical significance was established at $P < 0.05$.

3. Results

3.1. YAP expression is increased in CCl_4-induced liver fibrosis model mice and reduced upon fibrosis reversion

To evaluate the role of YAP in liver fibrosis activation and reversal, we first generated a CCl_4-induced liver fibrosis mouse model and recovery mouse model. The serum ALT and AST levels were elevated in the liver fibrosis mice and reduced in the recovery mice (Fig. 1A). In

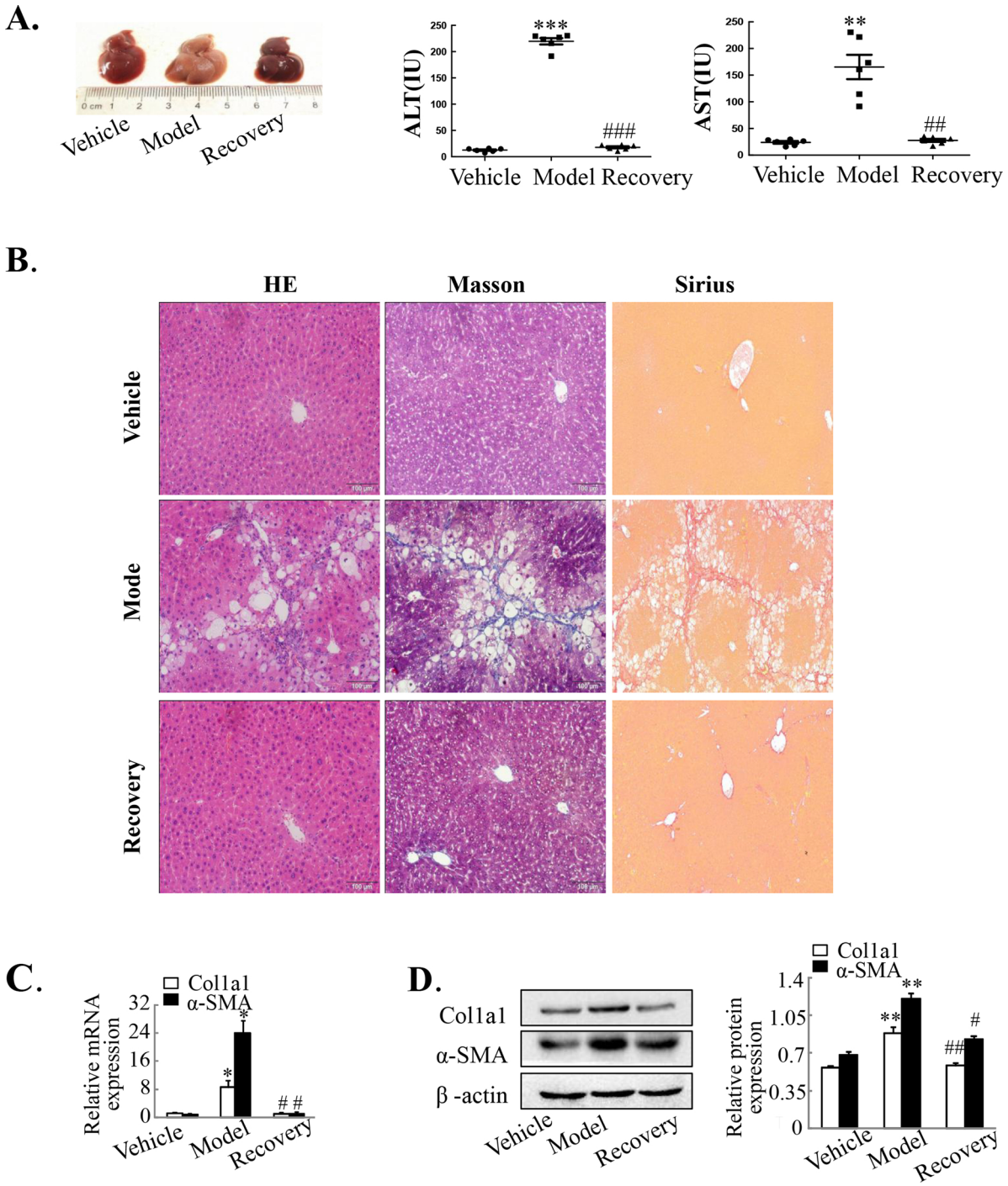

Fig. 1. YAP expression was increased in liver tissue from the hepatic fibrosis mice and decreased in spontaneous recovery, n = 15 mice/group. (A) The fresh livers from vehicle group, model group and recovery group mice before fixation. The serum ALT and AST were detected, $^{**}p < 0.01$, $^{***}p < 0.001$ vs vehicle and $\#\#p < 0.01$, $\#\#\#p < 0.001$ vs model. (B) Pathology observation of mice liver sections stained with hematoxylin and eosin (H&E) staining, Masson staining and Sirius red stain (×200). The mRNA and protein changes of Col1a1 and α-SMA in mice liver tissues were assessed by RT-PCR (C) and Western Blot (D), n = 6 mice/group, $^{*}p < 0.05$, $^{**}p < 0.01$ vs vehicle and $\#p < 0.05$, $\#\#p < 0.01$ vs model. The mRNA of YAP in primary HSCs and protein of YAP in tissues were analyzed (E–F), n = 6 mice/group, $^{**}p < 0.01$ vs vehicle and $\#\#p < 0.01$ vs model. (G) Double immunofluorescence staining of α-SMA (red) and YAP (green) in vehicle, model and recovery mice liver sections was performed, representative views were presented (×200).

addition, we investigated the degree of liver fibrosis in CCl_4-induced mice and recovery mice by histopathological studies. Hematoxylin and staining, Masson Trichrome staining and Sirius-Red staining revealed prominent hepatic steatosis, necrosis, fibrosis and collagen deposition in the liver fibrosis model (Fig. 1B). However, steatosis, necrosis and collagen deposition were reduced in the recovery mice compared with liver fibrosis mice. Furthermore, Col1a1 and α-SMA mRNA and protein expressions were up-regulated in liver tissue from the hepatic fibrosis mice and down-regulated in liver tissue from the recovery mice (Fig. 1C, D). Together these data confirmed the successful establishment of the CCl_4-induced liver fibrosis mouse model and recovery mouse model. The mRNA level of YAP was elevated in the primary cells of CCl_4-induced liver fibrosis and reduced in the recovery mice (Fig. 1E), western blot result showed that YAP protein had similar

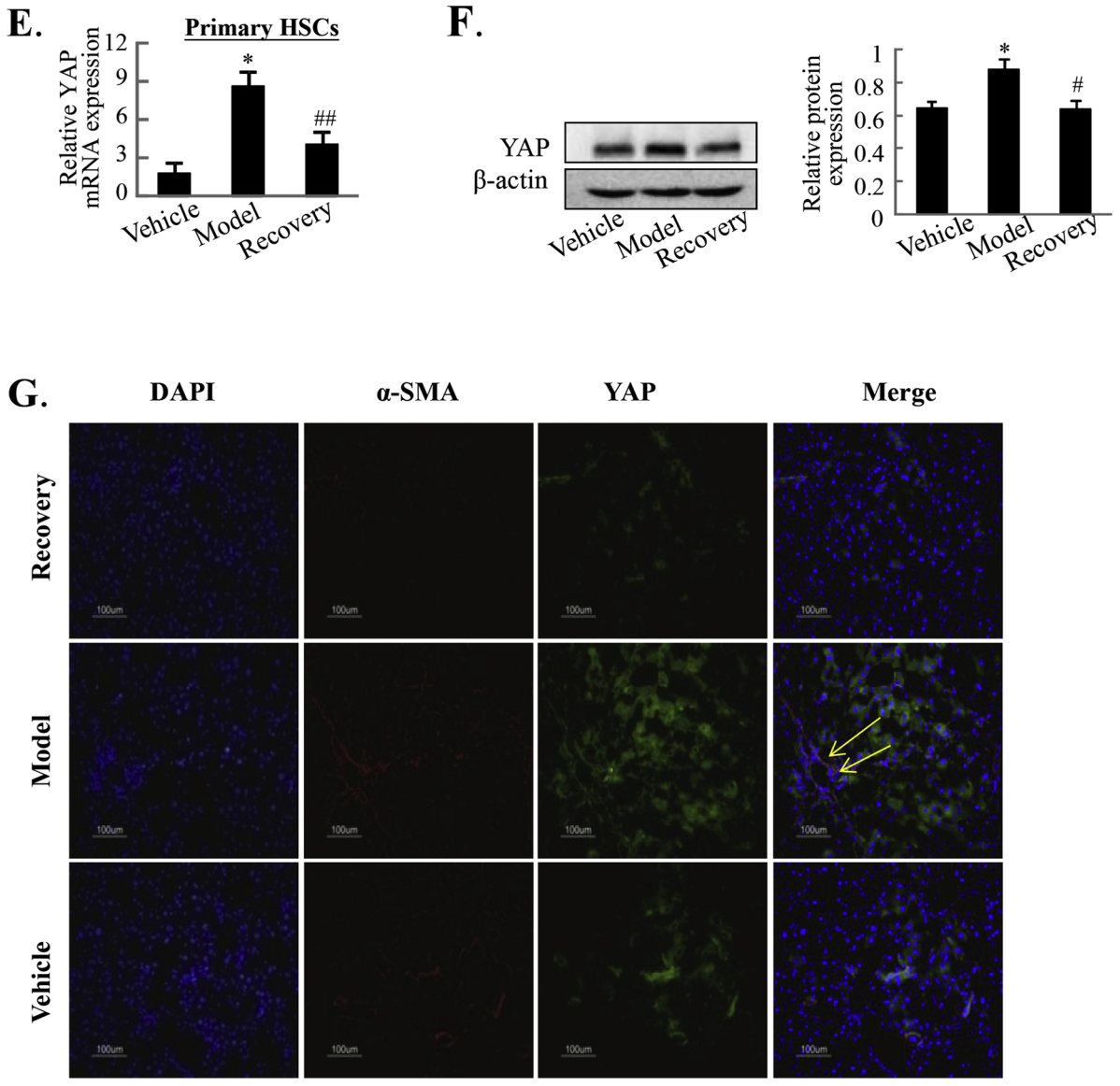

Fig. 1. (*continued*)

changes to the mRNA of primary cells in liver tissue (Fig. 1F). In addition, immunofluorescence staining showed that YAP co-localized with α-SMA in liver tissue of fibrosis mice (Fig. 1G). It also showed that YAP co-localized with desmin in mice liver (Supplemental Fig. 1).

3.2. YAP is elevated in TGF-β1-activated HSC-T6 cells and reduced in MDI-mediated inactivated HSC-T6 cells in vitro

In chronic liver injury, HSCs are activated and trans-differentiated into proliferative myofibroblast-like cells, which are significant in the development of liver fibrosis. HSC-T6 cells can be activated *in vitro* by TGF-β1. As shown in Fig. 2A, Col1a1 and α-SMA expressions were elevated in HSC-T6 cells treated with TGF-β1 (10 ng/ml) for 0, 12, 24 and 48 h. YAP expression also increased in response to TGF-β1 in a time-dependent manner. We next cultured activated HSC-T6 cells with MDI for 48 h to reverse the activation of these cells, as described previously (She et al., 2005; Wu et al., 2015). Both mRNA and protein expressions of Col1a1 and α-SMA were reduced after MDI treatment (Fig. 2B, C), indicating that the activated HSC-T6 cells successfully reverted *in vitro*. Both the mRNA and protein expressions of YAP were also reduced after MDI treatment for 48 h (Fig. 2D, E). These results indicated that YAP might be involved in the activation and reversion of HSCs *in vitro*.

3.3. YAP silencing inhibits HSC-T6 cell activation and proliferation, and promotes apoptosis of activated HSC-T6 cells

To explore the function of YAP *in vitro*, we used a specific siRNA targeting YAP to silence its expression (Fig. 3A, Supplemental Fig. 2A). Notably, YAP silencing in HSC-T6 cells treated with TGF-β1 inhibited the expression of CTGF mRNA (Supplemental Fig. 2B) and blocked the induction of Col1a1 and α-SMA protein expressions compared to the scrambled-siRNA group (Fig. 3B). This result indicated that Col1a1 and α-SMA expressions in activated HSC-T6 cells were inhibited by silencing YAP. Flow cytometric analysis showed that knockdown of YAP increased the percentage of cells in G0/G1 phase in activated HSC-T6 cells compared with HSC-T6 cells treated with scrambled-siRNA (Fig. 3C). Moreover, CCK-8 assay showed that YAP-siRNA reduced the viability of TGF-β1-treated HSC-T6 cells (Fig. 3D). We also found that early apoptosis was increased in activated cells transfected with YAP-siRNA compared with cells transfected with scrambled-siRNA (Fig. 3E). Western blot analysis further showed that knockdown of YAP upregulated the Bax/Bcl-2 ratio and cleaved caspase-3 (Fig. 3F). Together, these data showed that loss of YAP could inhibit HSC-T6 cells activation and proliferation and accelerate apoptosis of activated cells.

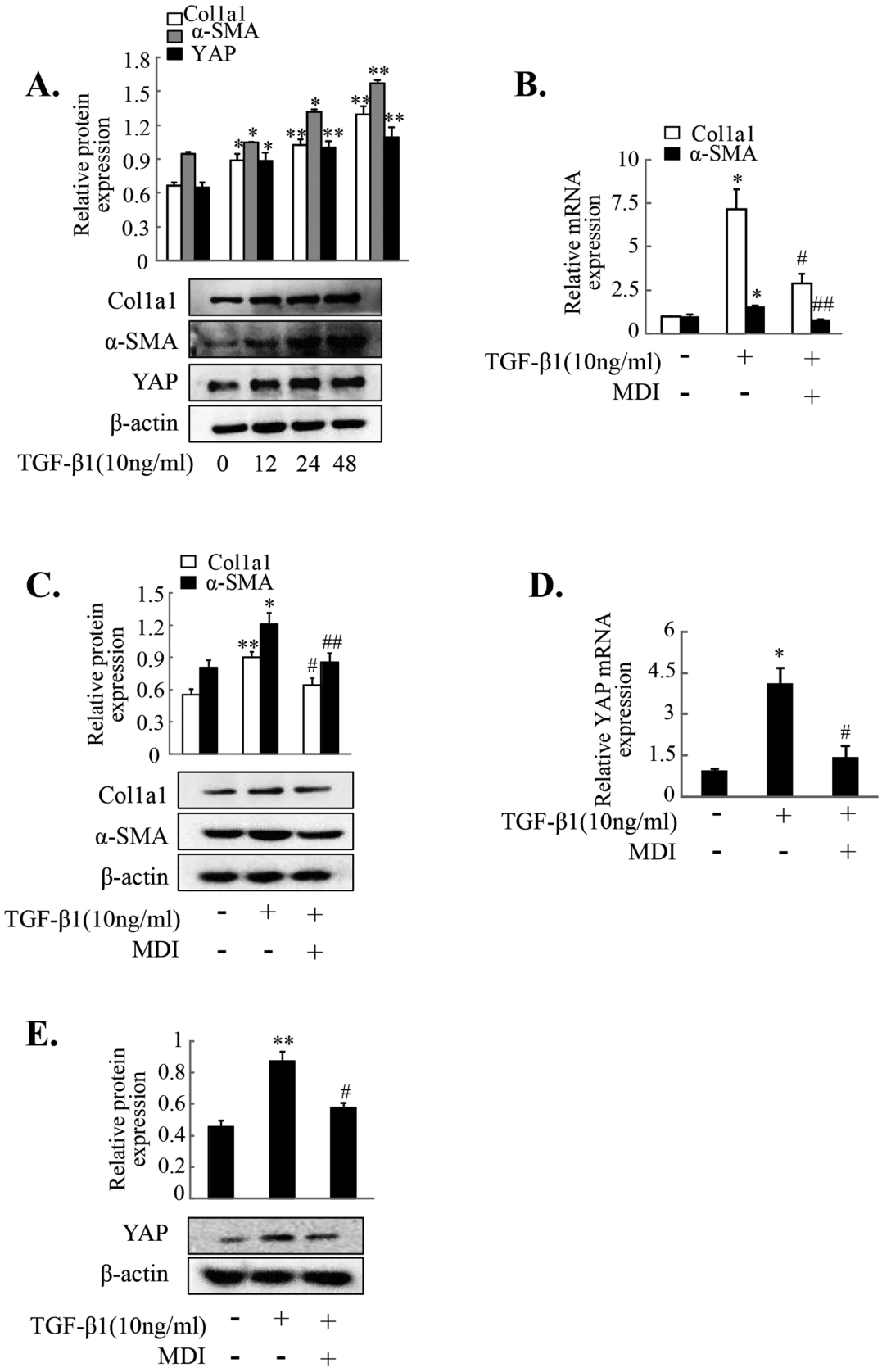

Fig. 2. YAP expression was increased in activated HSC-T6 cells and decreased in inactivated HSC-T6 cells induced by MDI. (A) HSC-T6 cells were activated by TGF-β1 (10 ng/ml) for 0, 12, 24, 48 h, the protein levels of Col1a1, α-SMA and YAP were examined, representative blots of three independent experiments are shown, $*p < 0.05$, $**p < 0.01$ vs 0 h. The mRNA and protein levels of Col1a1 and α-SMA in HSC-T6 cells treated by TGF-β1 (10 ng/ml) for 24 h and MDI for 48 h were assessed (B–C), $*p < 0.05$ vs control and $\#p < 0.05$, $\#\#p < 0.01$ vs TGF-β1. The YAP mRNA and protein were also changed after being assessed by RT-PCR (D) and Western Blot (E), $*p < 0.05$ control and $\#p < 0.05$ vs TGF-β1.

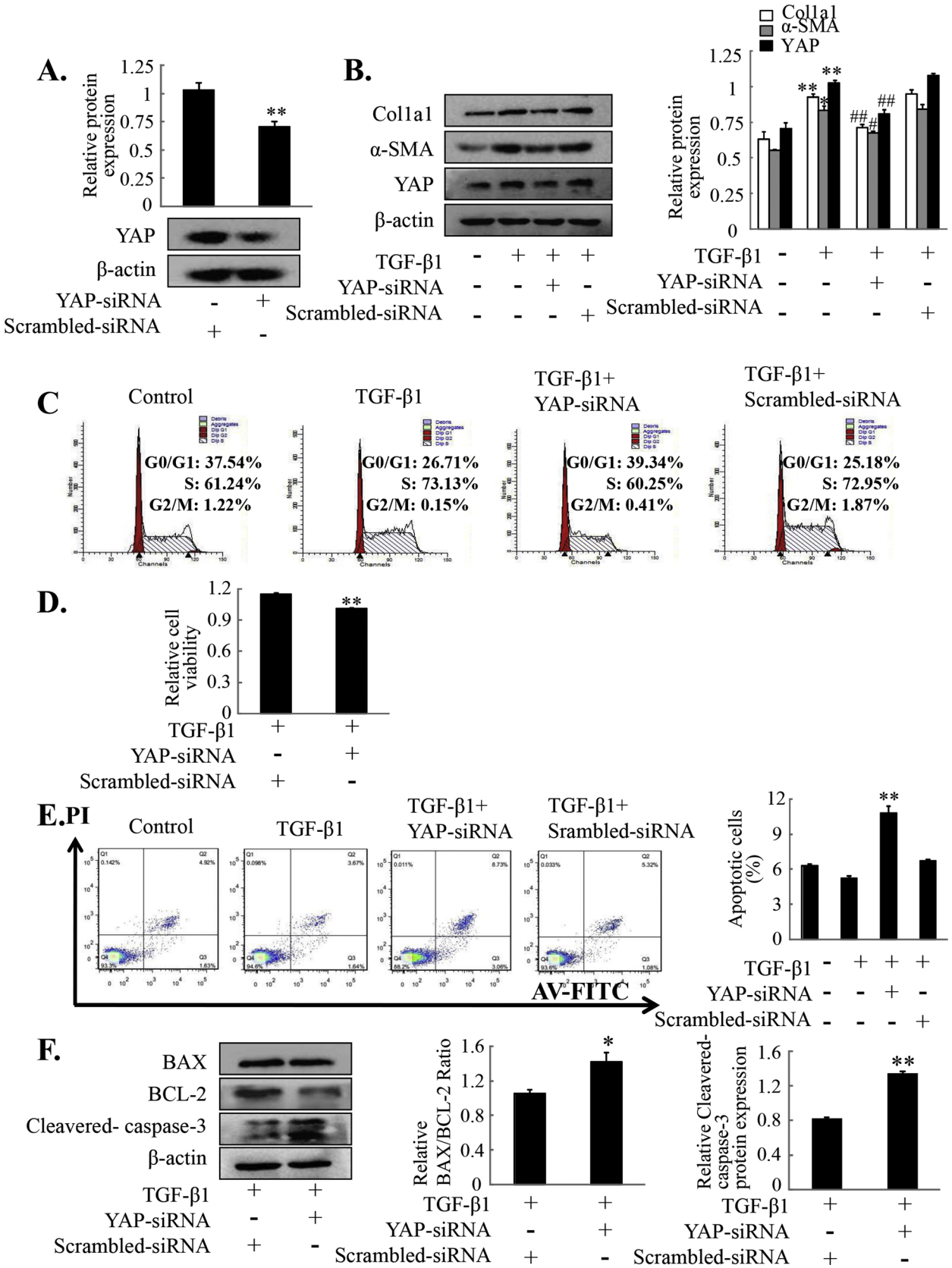

Fig. 3. Effect of YAP on activated HSC-T6 cells. (A) YAP in HSC-T6 cells was successfully inhibited by YAP-siRNA, $^{**}p < 0.01$ vs Scrambled-siRNA. (B) The proteins of Col1a1, α-SMA and YAP were examined after activated HSC-T6 cells being transfected with YAP-siRNA, $^{**}p < 0.01$ vs control and $\#p < 0.05$, $\#\#p < 0.01$ vs TGF-β1 + Scrambled-siRNA. (C) The cell cycle was analyzed after activated cell being treated with YAP-siRNA. (D) The cell viability of HSC-T6 cells after YAP-siRNA treatment was changed, $^{**}p < 0.01$ vs TGF-β1 + Scrambled-siRNA. (E) Cell apoptosis rate was detected by FACS analysis, $^{**}p < 0.01$ vs TGF-β1 + Scrambled-siRNA. (F) The protein levels of apoptosis associated proteins in the YAP-siRNA transfected HSC-T6 cells, such as Bcl-2, Bax and Cleaved-caspase3 were assessed, $^{**}p < 0.01$ vs TGF-β1 + Scrambled- siRNA.

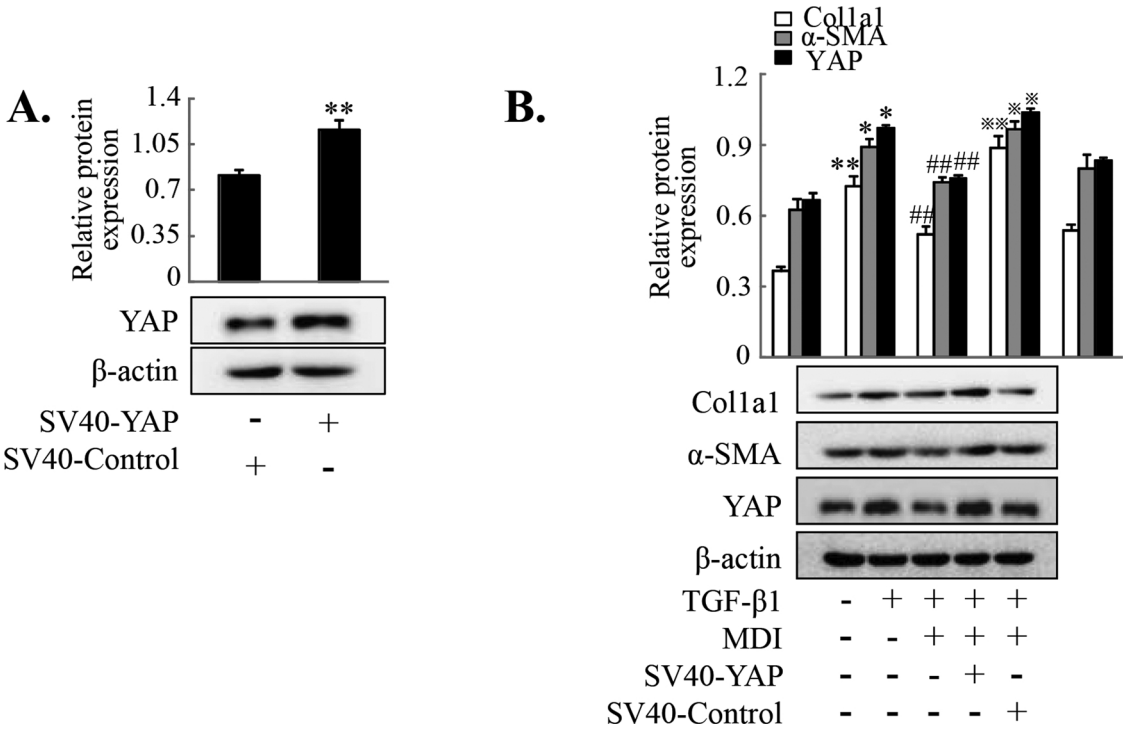

Fig. 4. MDI-induced HSC-T6 cells inactivation was reversed by plasmid SV40-YAP. (A) YAP was successfully over-expression after cells being treated with SV40-YAP. (B) The MDI-induced inactivated cells were treated with SV40-YAP, the protein levels of Col1a1, α-SMA and YAP were analyzed, $*p < 0.05$, $**p < 0.01$ vs control, $\#\#p < 0.01$ vs TGF-β1 and ※$p <$ 0.05, ※※$p < 0.01$ vs TGF-β1 + MDI + SV40-Control.

3.4. Over-expression of YAP blocks MDI-mediated reversion of activated HSC-T6 cells

To more closely examine the influence of YAP on the reversion of liver fibrosis, we used the SV40-YAP expression plasmid to up-regulate YAP expression in HSC-T6 cells. As shown in Fig. 4A, YAP was successfully up-regulated in HSC-T6 cells transfected with SV40-YAP. The Col1a1 and α-SMA were enhanced in MDI-mediated reversion of activated HSC-T6 cells after being transfected with SV40-YAP compared with being transfected with SV40-control (Fig. 4B). The expression of CTGF mRNA also was promoted after SV40-YAP treatment (Supplemental Fig. 2C).

3.5. YAP positively regulates the Wnt/β-catenin pathway in activated HSC-T6 cells and reversed cells

Previous studies showed that YAP interacts with the Wnt/β-catenin pathway in various diseases. As shown in Fig. 5A, β-catenin expression was up-regulated in liver fibrosis tissue from the mouse model and down-regulated to control levels in liver tissue of recovery mice. In addition, β-catenin was increased in activated HSC-T6 cells and decreased after MDI treatment (Fig. 5B). Interestingly, we found that the subcellular localization of YAP was altered in liver tissue and cells. YAP nuclear expression increased in liver tissue of hepatic fibrosis mice and decreased in fibrosis recovery, while cytoplasmic YAP had opposite changes from nuclear YAP (Supplemental Fig. 3). Moreover, changes in cellular localization of YAP in HSC-T6 cells were consistent with changes in tissues (Fig. 5C). These results indicated that activated YAP localized to the nucleus in TGF-β1-stimulated HSC-T6 cells and relocated to the cytoplasm during MDI treatment. We thus speculated that YAP activation promoted β-catenin expression. As shown in Fig. 5D, silencing of YAP in activated HSC-T6 cells resulted in reduced β-catenin protein expression. Other Wnt/β-catenin pathway downstream target genes, such as C-myc and cyclin D1 genes, showed similar changes in response to YAP silencing. Furthermore, over-expression of YAP in MDI-treated activated HSC-T6 cells recovered β-catenin, C-myc and cyclin D1 protein expressions compared with SV40-control (Fig. 5E). Together, these results indicated that YAP could positively regulate the Wnt/β-catenin pathwayin liver fibrosis development and recovery.

3.6. VP suppresses HSC-T6 cells activation and proliferation, and facilitates apoptosis of activated HSC-T6 cells

VP, YAP inhibitor, was used to confirm the effects in hepatic fibrosis progression and recovery. As shown in Supplemental Fig. 4A, VP improved hepatic steatosis, necrosis and collagen deposition in hepatic fibrosis mice, moreover, VP slightly enhanced the effect of spontaneously reversal of hepatic fibrosis on the recovery of hepatic steatosis, necrosis and collagen deposition. *In vitro*, we first examined the cytotoxicity of various concentrations of VP (0.25 mM, 0.5 mM, 1 mM, 2.5 mM) in HSC-T6 cells. MTT assays demonstrated that VP treatment at all of the tested concentrations showed no cytotoxicity in HSC-T6 cells (Fig. 6A). We thus selected 2.5 mM VP for subsequent experiments. We evaluated the inhibition of VP (2.5 mM) on activated HSC-T6 cells. After VP treatment, CTGF mRNA was reduced (Supplemental Fig. 4B), and Col1a1 and α-SMA protein expressions were also decreased compared with activated cells treated with DMSO (Fig. 6B). VP also affected the cell cycle and apoptosis levels in HSC-T6 cells. As shown in Fig. 6C, TGF-β1-induced cells were arrested in G0/G1 phase after VP treatment compared to DMSO-treated cells. Moreover, β-catenin expression was decreased upon VP treatment (Fig. 6D). We also found that VP increased apoptosis of activated cells (Fig. 6E). These results demonstrated that inhibition of YAP with VP could impact the activation, proliferation and apoptosis of activated HSC-T6 cells, which might be through affecting YAP-induced target gene expression.

4. Discussion

Liver fibrosis is a common progressive pathological process that occurs after extended liver injury. ECM deposition is a characteristic

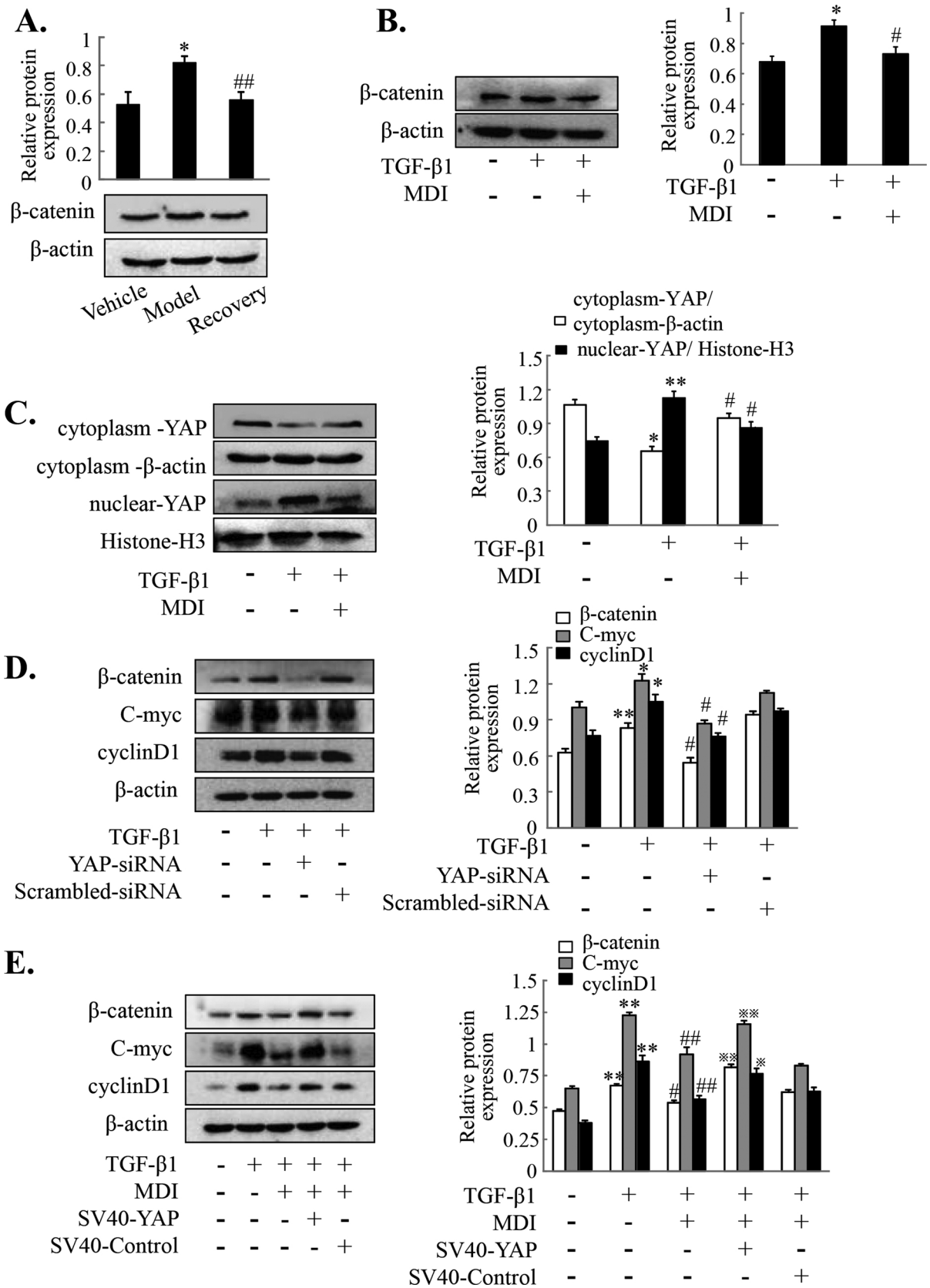

Fig. 5. The mechanism of YAP affecting HSC-T6 cells activation and proliferation. (A) β-catenin was examined in mice liver tissues, n = 6 mice/group, $^{**}p < 0.01$ vs vehicle and $\#\#p < 0.01$ vs model. (B) β-catenin also altered in HSC-T6 cells, $^{*}p < 0.05$ vs control, $\#p < 0.05$ vs TGF-β1. (C) The cytoplasmic and nuclear YAP protein levels changed in HSC-T6 cells activated by TGF-β1 and inactivated by MDI, $^{*}p < 0.05$, $^{**}p < 0.01$ vs control, $\#p < 0.05$ vs TGF-β1. (D) The protein levels of β-catenin, C-myc and CyclinD1 were detected after cells being transfected with YAP-siRNA, $^{*}p < 0.05$, $^{**}p < 0.01$ vs control, $\#p < 0.05$, $\#\#p < 0.01$ vs TGF-β1 + Scrambled-siRNA. (E) The protein levels of β-catenin, C-myc and CyclinD1 were assessed after MDI-induced inactivated HSC-T6 cells being treated with SV40-YAP, $^{*}p < 0.05$, $^{**}p < 0.01$ vs control, $\#p < 0.05$, $\#\#p < 0.01$ vs TGF-β1, $※p < 0.05$, $※※p < 0.01$ vs TGF-β1 + MDI + SV40-Control.

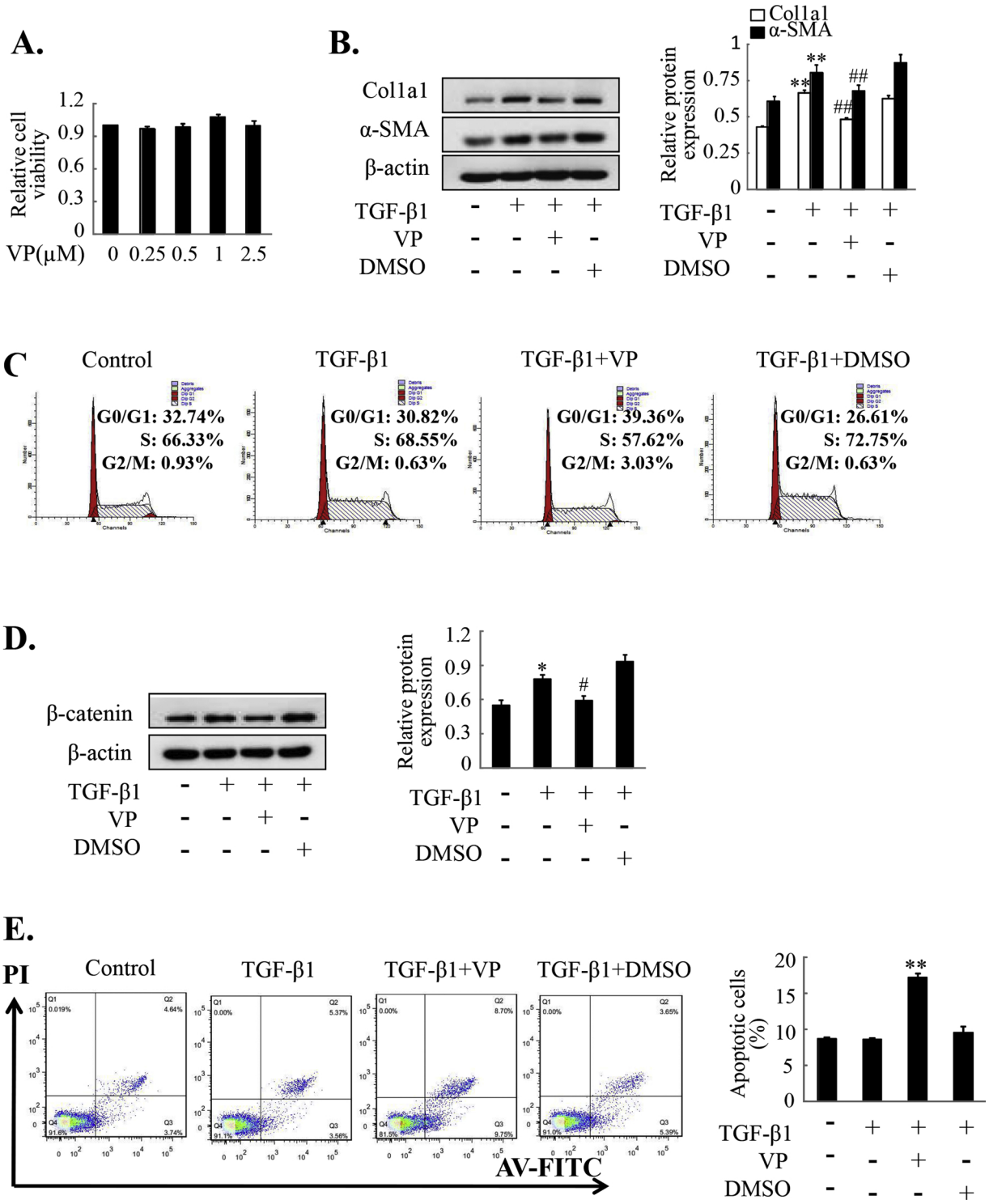

Fig. 6. HSC-T6 cells activation and proliferation were weakened by VP. (A) The cytotoxicity test of VP was achieved by MTT assay. (B) Col1a1 and α-SMA protein levels were analyzed in cells treated with VP, $^{**}p < 0.01$ vs control, $\#\#p < 0.01$ vs TGF-β1 + DMSO. (C) The impact of VP on activated HSC-T6 cells cycle. (D) The influence of VP on β-catenin protein expression, $^{**}p < 0.01$ vs control, $\#\#p < 0.01$ vs TGF-β1 + DMSO. (E) Cell apoptosis rate of VP-treated HSC-T6 cells was analyzed *via* FACS analysis, $^{**}p < 0.01$ vs TGF-β1 + DMSO.

feature of liver fibrosis, when hepatic stellate cells are activated, hepatic stellate cells proliferate and become the major producers of ECM. Therefore, repressing HSC activation and proliferation and promoting apoptosis have been focus for the treatment of liver fibrosis. During hepatic fibrosis reversion, the numbers of activated HSCs are reduced due to apoptosis or reversal to a quiescent state (Bedossa and Paradis, 2003). In addition, activation restriction, immune clearance and senescence may also be involved in the reduction of activated HSCs (Kong et al., 2013). Thus, accelerating the apoptosis and inactivation of activated HSCs can promote liver fibrosis recovery. In this study, YAP was increased in liver fibrosis tissue from a CCl_4-induced mouse model and in HSC-T6 cells activated by TGF-β1. In addition, YAP expression was decreased in liver tissue of recovery mice and MDI-mediated inactivated HSC-T6 cells. Notably, the levels of YAP expression were

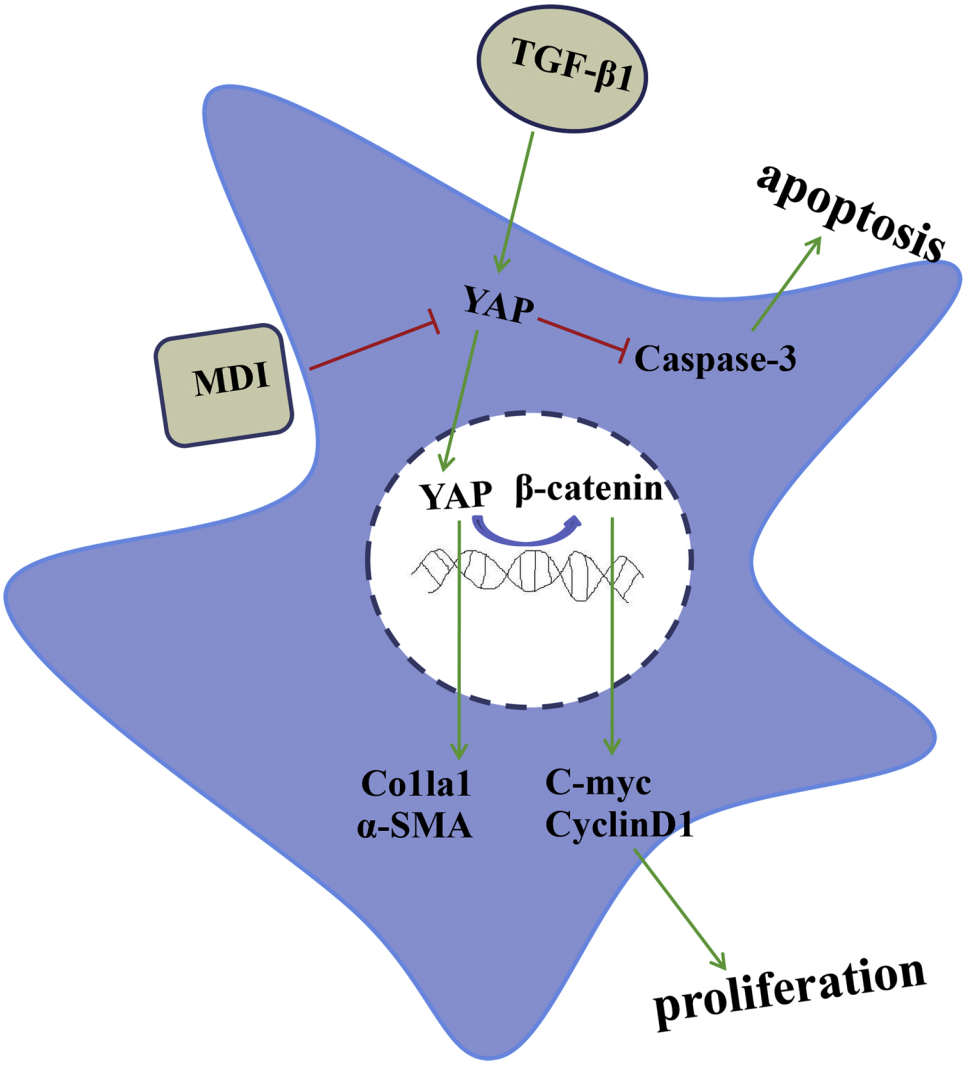

Fig. 7. Overview of YAP in hepatic fibrosis.

consistent with those of liver fibrosis markers (Col1a1 and α-SMA). These findings supported the potential involvement of YAP in liver fibrosis progression and reversion (Fig. 7).

Previous studies demonstrated that some components of the Hippo pathway, including YAP, are involved in the progression of many malignant tumors through their effects on cancer cell proliferation, apoptosis, migration and invasion (Harvey et al., 2013; Li et al., 2017; Liu et al., 2017). We thus speculated that YAP may play a role in HSC proliferation and apoptosis. YAP loss not only reduced Col1a1 and α-SMA levels but also reduced proliferation and promoted apoptosis of HSC-T6 cells stimulated by TGF-β1. The YAP-specific inhibitor VP also inhibited Col1a1 and α-SMA expressions, repressed the proliferation and increased apoptosis of activated cells. Previous studies found that YAP controlled HSC activation and pro-fibrotic factor expression at early liver fibrosis (Mannaerts et al., 2015). However, whether YAP performed the same function during liver fibrosis recovery had not been demonstrated. Our research indicates that over-expression of YAP could reverse the MDI-mediated inactivation of activated HSC-T6 cells. Together, our data suggest that YAP is essential in liver fibrosis progression and recovery.

Multiple studies have shown that the Wnt/β-catenin pathway is important for tumor cell proliferation and is involved in the progression of various cancers (Yang et al., 2018; MacDonald et al., 2009). In addition, the Wnt/β-catenin pathway is also critical for hepatic fibrosis (Miao et al., 2013), and β-catenin functions as a pro-fibrotic factor (Tan et al., 2011). Our laboratory also demonstrated that the Wnt/β-catenin pathway was activated and target genes such as C-myc and cyclinD1 genes were elevated in a CCl_4-induced liver fibrosis model and TGF-β1-induced HSC-T6 cells (Cai et al., 2016). Several studies have demonstrated a link between the Hippo/YAP pathway and Wnt/β-catenin pathway in various diseases. For instance, Yang et al found that blockage of YAP could reduce the proliferation of osteosarcoma cells through inhibiting the Wnt/β-catenin signaling pathway as well as C-myc and cyclin D1 gene expressions (Yang et al., 2014). Imajo et al showed that YAP could inhibit the expression of Wnt/β-catenin target genes through its binding β-catenin in the nucleus, and phosphorylated YAP could retain β-catenin in the cytoplasm to suppress the Wnt/β-catenin pathway (Imajo et al., 2012). Wnt/β-catenin pathway was also shown to influence the Hippo/YAP pathway. One study showed that β-catenin binds TCF4 to regulate YAP expression through interacting with the YAP promoter and impact YAP target gene expression in colorectal carcinoma cells (Konsavage et al., 2012). In addition, there was also alternative Wnt pathway that activated YAP/TAZ, not through canonical Wnt pathway, meanwhile, YAP/TAZ was mediators of this alternative Wnt pathway (Park et al., 2015). In the current study, we explored the interaction between YAP and Wnt/β-catenin. We found that β-catenin was increased in hepatic fibrosis and decreased in hepatic fibrosis recovery. We also showed that YAP was activated and translocated from the cytoplasm to the nucleus in HSC-T6 cells after TGF-β1 treatment, and this process was inhibited after MDI treatment. These

results indicated that YAP was stimulated in activated cells and suppressed in recovered cells. Thus, we suspected that YAP activation promoted β-catenin expression. We found that loss of YAP inhibited Wnt/β-catenin activity in activated HSC-T6 cells. In addition, VP, the YAP inhibitor, also repressed β-catenin expression. YAP over-expression enhanced Wnt/β-catenin pathway activation in MDI-mediated inactivated HSC-T6 cells. These findings indicate that activated YAP plays a critical role in hepatic fibrosis and recovery by positively regulating the Wnt/β-catenin pathway.

Our study suggested that blockade of YAP relieves hepatic fibrosis progression and accelerates regression of live fibrosis. However, the precise function of YAP in hepatic fibrosis development and reversion is not yet fully clear and requires more research. More studies are also required to elucidate the mechanism by which YAP regulates β-catenin localization as well as the effect of β-catenin on YAP activity.

Conflicts of interest

The authors declare there is no conflict of interest.

Acknowledgement

The project was supported by the National Science Foundation of China (No. 81473268)

Appendix A. Supplementary data

Supplementary material related to this article can be found, in the online version, at doi:https://doi.org/10.1016/j.molimm.2019.01.004.

References

Bedossa, P., Paradis, V., 2003. Approaches for treatment of liver fibrosis in chronic hepatitis C. Clin. Liver Dis. 7 (1), 195–210.
Bejoy, J., Song, L., Zhou, Y., Li, Y., 2018. Wnt/Yes-associated protein interactions during neural tissue patterning of human induced pluripotent stem cells. Tissue Eng. Part A 24 (7-8), 546–558.
Cai, S.P., Cheng, X.Y., Chen, P.J., Pan, X.Y., Xu, T., Huang, C., Meng, X.M., Li, J., 2016. Transmembrane protein 88 attenuates liver fibrosis by promoting apoptosis and reversion of activated hepatic stellate cells. Mol. Immunol. 80, 58–67.
Deng, F., Peng, L., Li, Z., Tan, G., Liang, E., Chen, S., Zhao, X., Zhi, F., 2018. YAP triggers the Wnt/beta-catenin signalling pathway and promotes enterocyte self-renewal, regeneration and tumorigenesis after DSS-induced injury. Cell Death Dis. 9 (2), 153.
Ellis, E.L., Mann, D.A., 2012. Clinical evidence for the regression of liver fibrosis. J. Hepatol. 56 (5), 1171–1180.
Grijalva, J.L., Huizenga, M., Mueller, K., Rodriguez, S., Brazzo, J., Camargo, F., Sadri-Vakili, G., Vakili, K., 2014. Dynamic alterations in Hippo signaling pathway and YAP activation during liver regeneration. Am. J. Physiol. Gastrointest. Liver Physiol. 307 (2), G196–204.
Halder, G., Johnson, R.L., 2011. Hippo signaling: growth control and beyond. Development 138 (1), 9–22.
Harvey, K.F., Zhang, X., Thomas, D.M., 2013. The Hippo pathway and human cancer. Nat. Rev. Cancer 13 (4), 246–257.
Heallen, T., Zhang, M., Wang, J., Bonilla-Claudio, M., Klysik, E., Johnson, R.L., Martin, J.F., 2011. Hippo pathway inhibits Wnt signaling to restrain cardiomyocyte proliferation and heart size. Science 332 (6028), 458–461.
Imajo, M., Miyatake, K., Iimura, A., Miyamoto, A., Nishida, E., 2012. A molecular mechanism that links Hippo signalling to the inhibition of Wnt/beta-catenin signalling. EMBO J. 31 (5), 1109–1122.
Kong, D., Zhang, F., Zhang, Z., Lu, Y., Zheng, S., 2013. Clearance of activated stellate cells for hepatic fibrosis regression: molecular basis and translational potential. Biomed. Pharmacother. 67 (3), 246–250.
Konishi, T., Schuster, R.M., Lentsch, A.B., 2018. Proliferation of hepatic stellate cells, mediated by YAP and TAZ, contributes to liver repair and regeneration after liver ischemia-reperfusion injury. Am. J. Physiol. Gastrointest. Liver Physiol. 314 (4), G471–G482.
Konsavage Jr., W.M., Kyler, S.L., Rennoll, S.A., Jin, G., Yochum, G.S., 2012. Wnt/beta-catenin signaling regulates Yes-associated protein (YAP) gene expression in colorectal carcinoma cells. J. Biol. Chem. 287 (15), 11730–11739.
Li, H., Huang, Z., Gao, M., Huang, N., Luo, Z., Shen, H., Wang, X., Wang, T., Hu, J., Feng, W., 2016. Inhibition of YAP suppresses CML cell proliferation and enhances efficacy of imatinib in vitro and in vivo. J. Exp. Clin. Cancer Res. 35 (1), 134.
Li, H., He, F., Zhao, X., Zhang, Y., Chu, X., Hua, C., Qu, Y., Duan, Y., Ming, L., 2017. YAP inhibits the apoptosis and migration of human rectal Cancer cells via suppression of JNK-Drp1-Mitochondrial Fission-HtrA2/Omi pathways. Cell. Physiol. Biochem. 44 (5), 2073–2089.
Liu, Z., Zeng, W., Wang, S., Zhao, X., Guo, Y., Yu, P., Yin, X., Liu, C., Huang, T., 2017. A potential role for the Hippo pathway protein, YAP, in controlling proliferation, cell cycle progression, and autophagy in BCPAP and KI thyroid papillary carcinoma cells. Am. J. Transl. Res. 9 (7), 3212–3223.
MacDonald, B.T., Tamai, K., He, X., 2009. Wnt/beta-catenin signaling: components, mechanisms, and diseases. Dev. Cell 17 (1), 9–26.
Machado, M.V., Michelotti, G.A., Pereira, T.A., Xie, G., Premont, R., Cortez-Pinto, H., Diehl, A.M., 2015. Accumulation of duct cells with activated YAP parallels fibrosis progression in non-alcoholic fatty liver disease. J. Hepatol. 63 (4), 962–970.
Mannaerts, I., Leite, S.B., Verhulst, S., Claerhout, S., Eysackers, N., Thoen, L.F., Hoorens, A., Reynaert, H., Halder, G., van Grunsven, L.A., 2015. The Hippo pathway effector YAP controls mouse hepatic stellate cell activation. J. Hepatol. 63 (3), 679–688.
Miao, C.G., Yang, Y.Y., He, X., Huang, C., Huang, Y., Zhang, L., Lv, X.W., Jin, Y., Li, J., 2013. Wnt signaling in liver fibrosis: progress, challenges and potential directions. Biochimie 95 (12), 2326–2335.
Miyamura, N., Hata, S., Itoh, T., Tanaka, M., Nishio, M., Itoh, M., Ogawa, Y., Terai, S., Sakaida, I., Suzuki, A., et al., 2017. YAP determines the cell fate of injured mouse hepatocytes in vivo. Nat. Commun. 8, 16017.
Oh, H., Irvine, K.D., 2010. Yorkie: the final destination of Hippo signaling. Trends Cell Biol. 20 (7), 410–417.
Ou, C., Sun, Z., Li, S., Li, G., Li, X., Ma, J., 2017. Dual roles of yes-associated protein (YAP) in colorectal cancer. Oncotarget 8 (43), 75727–75741.
Park, H.W., Kim, Y.C., Yu, B., Moroishi, T., Mo, J.S., Plouffe, S.W., Meng, Z., Lin, K.C., Yu, F.X., Alexander, C.M., et al., 2015. Alternative wnt signaling activates YAP/TAZ. Cell 162 (4), 780–794.
Parola, M., Marra, F., Pinzani, M., 2008. Myofibroblast - like cells and liver fibrogenesis: emerging concepts in a rapidly moving scenario. Mol. Aspects Med. 29 (1-2), 58–66.
She, H., Xiong, S., Hazra, S., Tsukamoto, H., 2005. Adipogenic transcriptional regulation of hepatic stellate cells. J. Biol. Chem. 280 (6), 4959–4967.
Shi, X., Zhu, H.R., Liu, T.T., Shen, X.Z., Zhu, J.M., 2017. The Hippo pathway in hepatocellular carcinoma: non-coding RNAs in action. Cancer Lett. 400, 175–182.
Si, H.F., Lv, X., Guo, A., Jiang, H., Li, J., 2008. Suppressive effect of leflunomide on rat hepatic stellate cell proliferation involves on PDGF-BB-elicited activation of three mitogen-activated protein kinases. Cytokine 42 (1), 24–31.
Sudol, M., Bork, P., Einbond, A., Kastury, K., Druck, T., Negrini, M., Huebner, K., Lehman, D., 1995. Characterization of the mammalian YAP (Yes-associated protein) gene and its role in defining a novel protein module, the WW domain. J. Biol. Chem. 270 (24), 14733–14741.
Tan, R.J., Zhou, D., Zhou, L., Liu, Y., 2011. Wnt/beta-catenin signaling and kidney fibrosis. Kidney Int. Suppl. (2011) 4 (1), 84–90 2014.
Wang, Y., Pan, P., Wang, Z., Zhang, Y., Xie, P., Geng, D., Jiang, Y., Yu, R., Zhou, X., 2017. Beta-catenin-mediated YAP signaling promotes human glioma growth. J. Exp. Clin. Cancer Res. 36 (1), 136.
Wu, Y., Liu, X., Zhou, Q., Huang, C., Meng, X., Xu, F., Li, J., 2015. Silent information regulator 1 (SIRT1) ameliorates liver fibrosis via promoting activated stellate cell apoptosis and reversion. Toxicol. Appl. Pharmacol. 289 (2), 163–176.
Wu, H., Liu, Y., Jiang, X.W., Li, W.F., Guo, G., Gong, J.P., Ding, X., 2016. Clinicopathological and prognostic significance of Yes-associated protein expression in hepatocellular carcinoma and hepatic cholangiocarcinoma. Tumour Biol. 37 (10), 13499–13508.
Yang, Z., Zhang, M., Xu, K., Liu, L., Hou, W.K., Cai, Y.Z., Xu, P., Yao, J.F., 2014. Knockdown of YAP1 inhibits the proliferation of osteosarcoma cells in vitro and in vivo. Oncol. Rep. 32 (3), 1265–1272.
Yang, B., Sun, H., Song, F., Yu, M., Wu, Y., Wang, J., 2017. YAP1 negatively regulates chondrocyte differentiation partly by activating the β-catenin signaling pathway. Int. J. Biochem. Cell Biol. 87, 104–113.
Yang, M., Wang, M., Li, X., Xie, Y., Xia, X., Tian, J., Zhang, K., Tang, A., 2018. Wnt signaling in cervical cancer? J. Cancer 9 (7), 1277–1286.
Yu FX, Zhao B., Guan, K.L., 2015. Hippo pathway in organ size control, tissue homeostasis, and Cancer. Cell 163 (4), 811–828.
Zhang, D., Zhuang, R., Guo, Z., Gao, M., Huang, L., You, L., Zhang, P., Li, J., Su, X., Wu, H., et al., 2018. Desmin- and vimentin-mediated hepatic stellate cell-targeting radiotracer (99m)Tc-GlcNAc-PEI for liver fibrosis imaging with SPECT. Theranostics 8 (5), 1340–1349.